S108

EUROPEAN ORGANIZATION FOR NUCLEAR RESEARCH

For internal circulation only

NP Internal Report 70-8
18 March 1970

TEST MEASUREMENT OF NEUTRON-PROTON CHARGE-EXCHANGE IN COINCIDENCE

J. Engler

ABSTRACT

A coincidence test measurement was carried out in order to investigate the possibility of using the whole neutron spectrum coming from an internal Be-target in an n-p charge exchange experiment. For recoil-neutron energies of 1-10 MeV, elastic peaks in the time-of-flight spectrum were clearly separated from the inelastic background.

Suggestions are given on how to extend the method to higher momentum transfers.

GENEVA
1970

This letter reports on the result of an attempt to measure the neutron-proton charge-exchange scattering in coincidence. In addition to the forward scattered proton, whose momentum and scattering angle were measured in a magnetic spectrometer, the recoil neutron was detected. Since the interesting peak in the forward direction decreases rapidly with momentum transfer, the neutrons to be detected have very low energies. Figure 1 shows the charge-exchange cross-sections as measured by Manning et al.[1] for 8 GeV neutrons. As can be seen from this figure it would be advisable to detect the recoil neutrons with a kinetic energy down to 1 MeV. The question arises then whether it is sufficient for the separation of the elastic scattering events from inelastic background to measure only the neutron time-of-flight on the neutron side.

Figure 2 shows the set-up of the neutron detector. The counter was a scintillator block of $30 \times 80 \times 300\ mm^3$, viewed by two photomultipliers. Zero cross-over discriminators were used in order to achieve a good time resolution, in spite of the fact that the pulse height spectrum begins just at the discriminator threshold (see Fig. 3).

P.J. Kurz[2] has written a program which calculates the detection efficiency of a plastic scintillator for neutrons using all known cross-sections of neutron-proton and neutron-carbon scattering. According to these calculations one has to set the discriminator threshold at 0.1 MeV electron energy in order to detect 1 MeV neutrons. This low threshold is caused mainly by the fact that the low-energy recoil protons produce less light in a scintillator than electrons of the same energy. The efficiency for this threshold and the block size used as calculated by the Kurz program is plotted in Fig. 4. One notices that at low neutron energies the efficiency varies strongly with energy, and that this variation depends critically on the detection threshold. For this provisional experiment the threshold of 0.1 MeV electron energy was set by using the Compton edges of the ^{137}Cs and ^{60}Co gamma-rays for calibration. The stability of the threshold was checked during the running time of about three days by repeating the calculation several times.

In order to determine the proper time-of-flight, the path length of the neutron must be known. The neutron recoil angle was calculated by assuming that all the protons which were accepted by the spectrometer resulted from elastic scattering. Furthermore, the travelling time of the light in the scintillator had to be taken into account. For this purpose, the interaction point in the scintillator block was determined by the time difference of the arrival of the light at both photomultipliers. A travelling time of 7.4 nsec/m was measured and a local resolution of ±2 cm FWHM was achieved.

In the time-of-flight spectrum of all detected events for intervals of different momentum transfer, the elastic peak was contaminated by a high background. As an example, the spectrum for events with a momentum transfer corresponding to 3-5 MeV neutrons is shown in Fig. 5. The contamination is mainly due to the fact that the bulk of the coincidences are caused by gamma-rays, which produce pulses of up to 12 MeV energy loss in the scintillator (see Fig. 6).

To extract better the elastic neutron events the following three restrictions were imposed: (a) the requirement that an elastic scattering event must fulfil the coplanarity constraint, that is in our case the proton azimuth angle had to be within $\pm 7^\circ$ (b) appropriate upper limits for the scintillator pulse heights (see Fig. 3) [these limits for the different neutron energies were obtained successively] and (c) the requirement that the neutron interaction point as determined by the time difference in the arrival at the photomultipliers lies within the scintillator. This last restriction is not trivial for low pulse heights, which can refer to Čerenkov light produced in the light guides.

Due to these three requirements the background in the time-of-flight spectra disappears; the resulting spectra are plotted in Fig. 7 and Fig. 8. The arrows indicate where the appropriate time-of-flight for the different neutron energies are expected. Elastic events could be separated from inelastic events for neutron energies of 1-10 MeV. Figure 9, on the other hand, shows the distribution of the azimuthal angles for events with the proper time-of-flight. One notices that the coplanarity has an unexpectedly broad distribution. This may have its origin in elastic scattering of the neutrons when traversing the target and the anticounter.

For neutron energies higher than 10 MeV the time resolution of ±2 nsec was not sufficient to separate the neutron time-of-flight from prompt coincidences of gamma events. For a future experiment three essential improvements are suggested:

a) installation of a second anticounter behind the neutron counter in order to veto gamma events, which produce large penetrating showers, whereas the recoil protons of the neutron events stop in the counter because of their short range;

b) using a longer distance for the flight and improvement of the zero cross-over discriminator, because the one used had not a sufficiently large dynamic range in pulse height acceptance; and

c) using a smaller hydrogen target and a very thin anticounter in front of the neutron counter in order not to lose elastic events by absorption and not to deflect the penetrating neutrons by elastic scattering.

REFERENCES

1) G. Manning, A. Parham, J.D. Jafar, H.B. van der Raay, D.H. Reading, D.G. Ryan, B.D. Jones, J. Malos and N.H. Lipman, Nuovo Cimento, 41A, 167 (1966).

2) P.J. Kurz, UCRL 11339, Berkeley, 1964.

Figure captions

Fig. 1 : The (n-p) charge-exchange cross-sections at 8 GeV primary kinetic energy as measured by Manning et al.[1]. The straight line represents the slope extrapolated from values of higher momentum transfer.

Fig. 2 : The set-up of the neutron counter with respect to the beam. The scintillator is viewed by two photomultipliers MP1 and MP2. a) Top view. b) Side view in direction of the beam.

Fig. 3 : The spectra of pulse heights in a plastic scintillator caused by neutrons of 1-7 MeV. The energy loss of an electron of the appropriate energy is chosen as the pulse-height scale. Calibration was done with the Compton edges of ^{137}Cs and ^{60}Co; the discriminator threshold was set at 0.1 MeV electron energy.

Fig. 4 : The detection efficiency of a plastic scintillator for neutrons of a thickness of 3 cm and a threshold corresponding to 0.1 MeV electron energy as calculated by the program of P.J. Kurz[2].

Fig. 5 : Time-of-flight spectra with no restrictions of events with momentum transfer corresponding to 3-5 MeV neutrons.

Fig. 6 : The spectrum of the pulse heights of all detected events. The energy scale is the same as that in Fig. 3.

Fig. 7 and Fig. 8 : Time-of-flight spectra for coplanar events with pulse-height limitation.

Fig. 9 : Distribution of the proton azimuth angle for neutrons with the proper time-of-flight of an elastic scattering event and limited pulse height. The geometrical possible acceptance at $\pm 7^{\circ}$ is indicated by two lines.

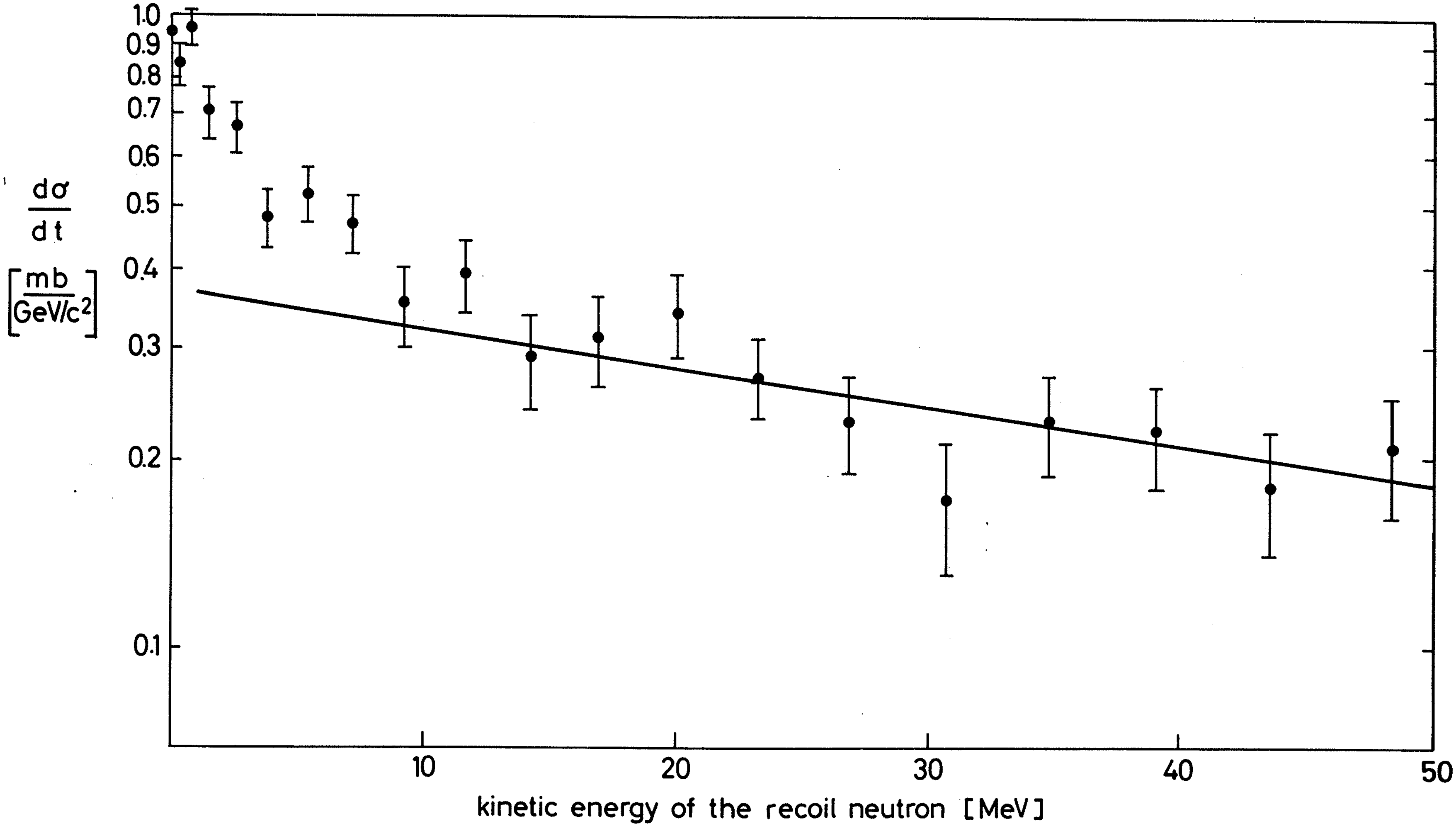
dσ/dt [mb/GeV/c²]
1.0
0.9
0.8
0.7
0.6
0.5
0.4
0.3
0.2
0.1
10
20
30
40
50
kinetic energy of the recoil neutron [MeV]

Fig. 1

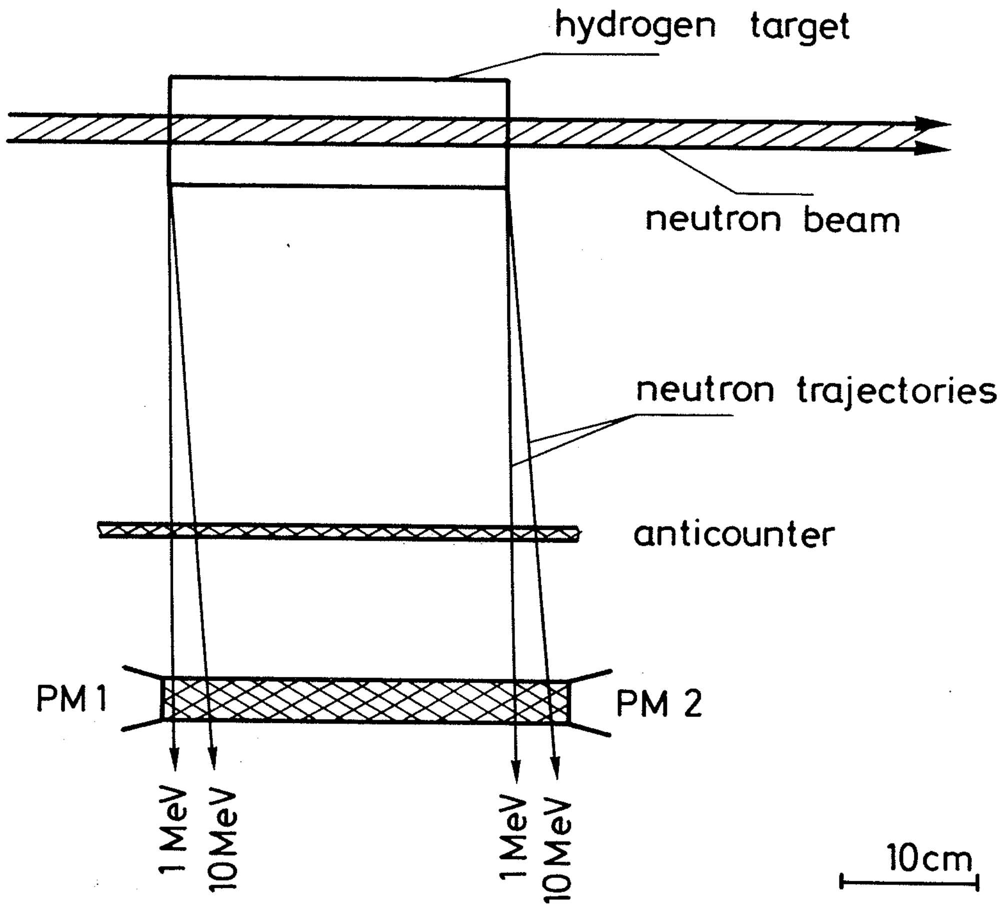
hydrogen target
neutron beam
neutron trajectories
anticounter
PM 1
PM 2
1 MeV
10 MeV
1 MeV
10 MeV
10cm

a)

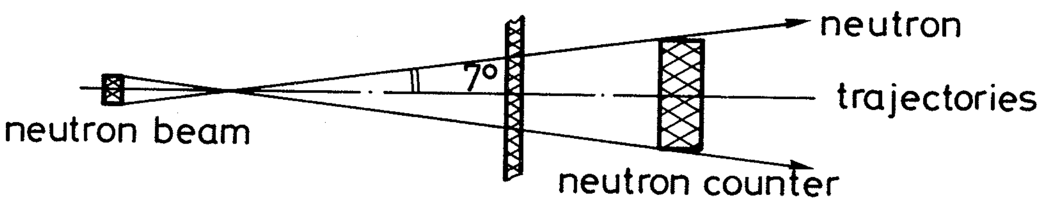
neutron
7°
trajectories
neutron beam
neutron counter

b)

Fig. 2

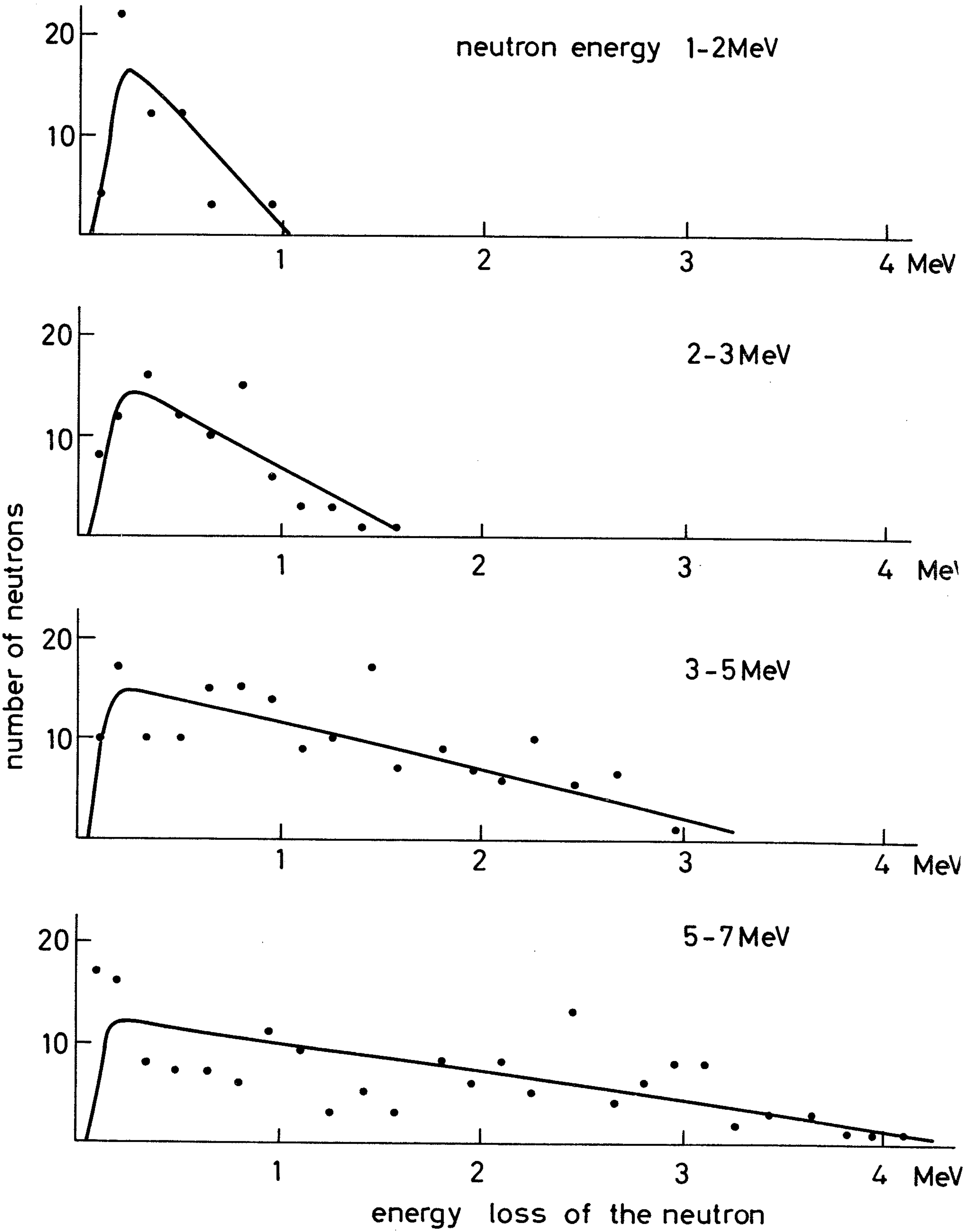

neutron energy 1-2MeV
2-3MeV
3-5MeV
5-7MeV
number of neutrons
energy loss of the neutron
20
10
1
2
3
4 MeV

Fig. 3

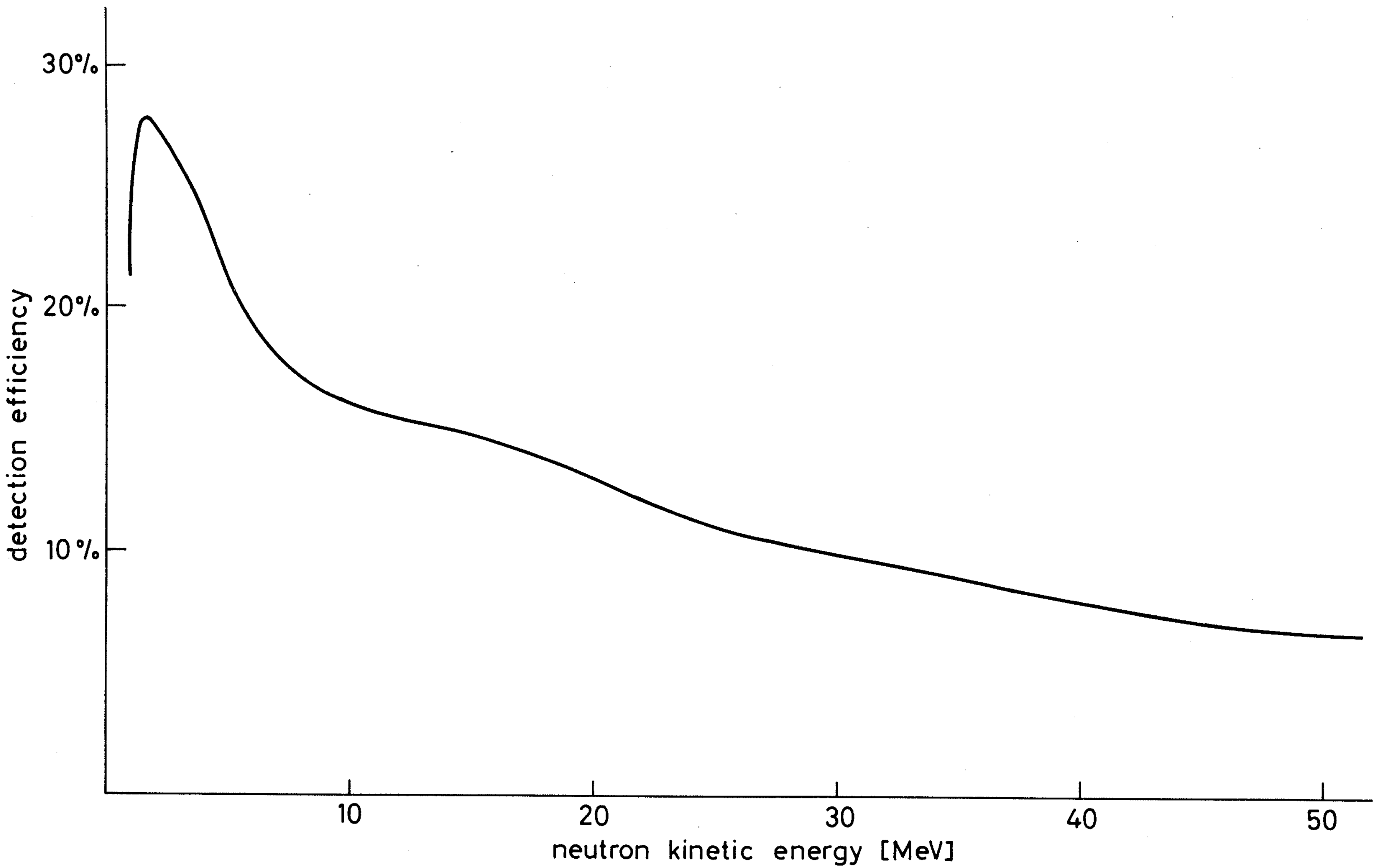
30%
20%
10%
detection efficiency
10
20
30
40
50
neutron kinetic energy [MeV]

Fig. 4

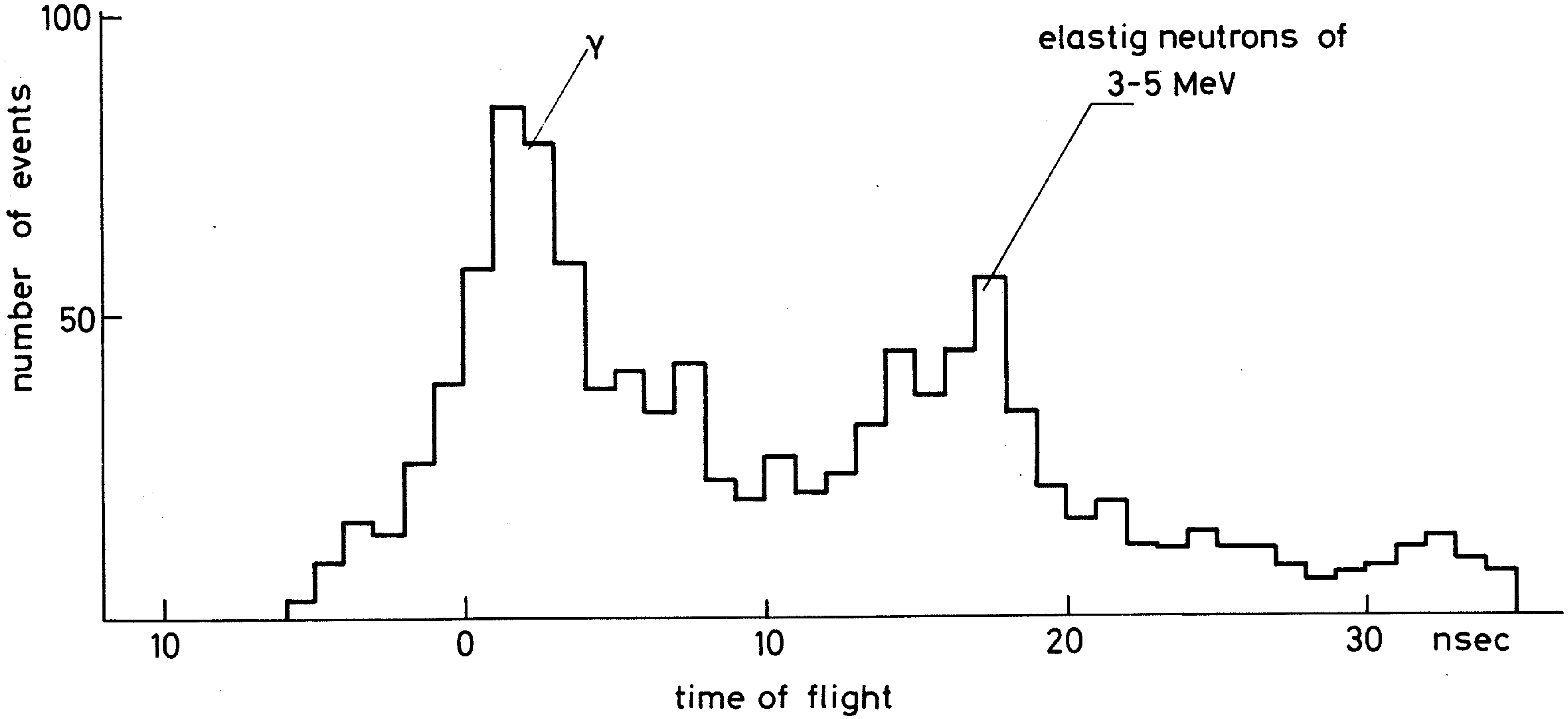
100
50
number of events
γ
elastig neutrons of
3-5 MeV
10
0
10
20
30
nsec
time of flight

Fig. 5

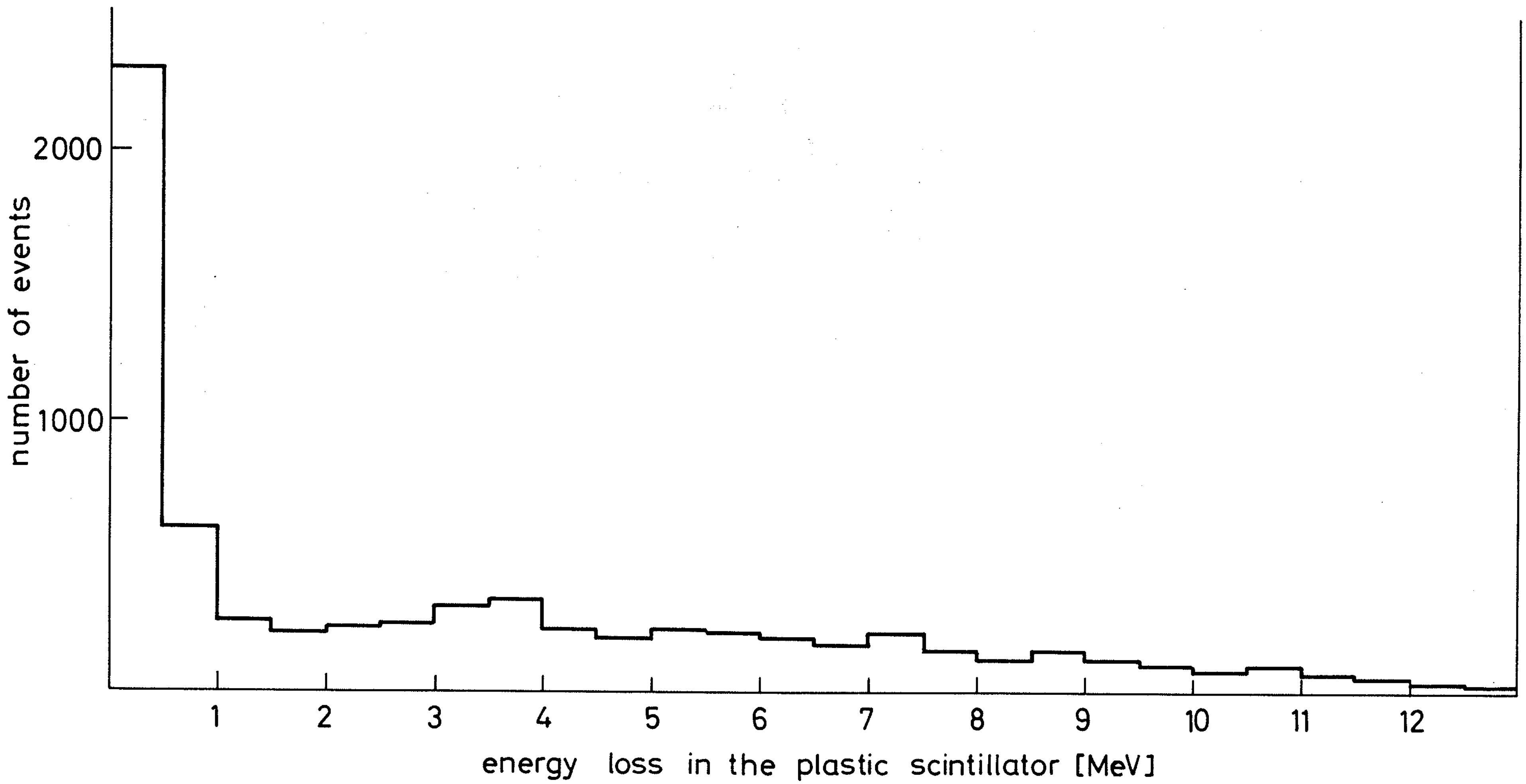

2000
1000
number of events
1
2
3
4
5
6
7
8
9
10
11
12
energy loss in the plastic scintillator [MeV]

Fig. 6

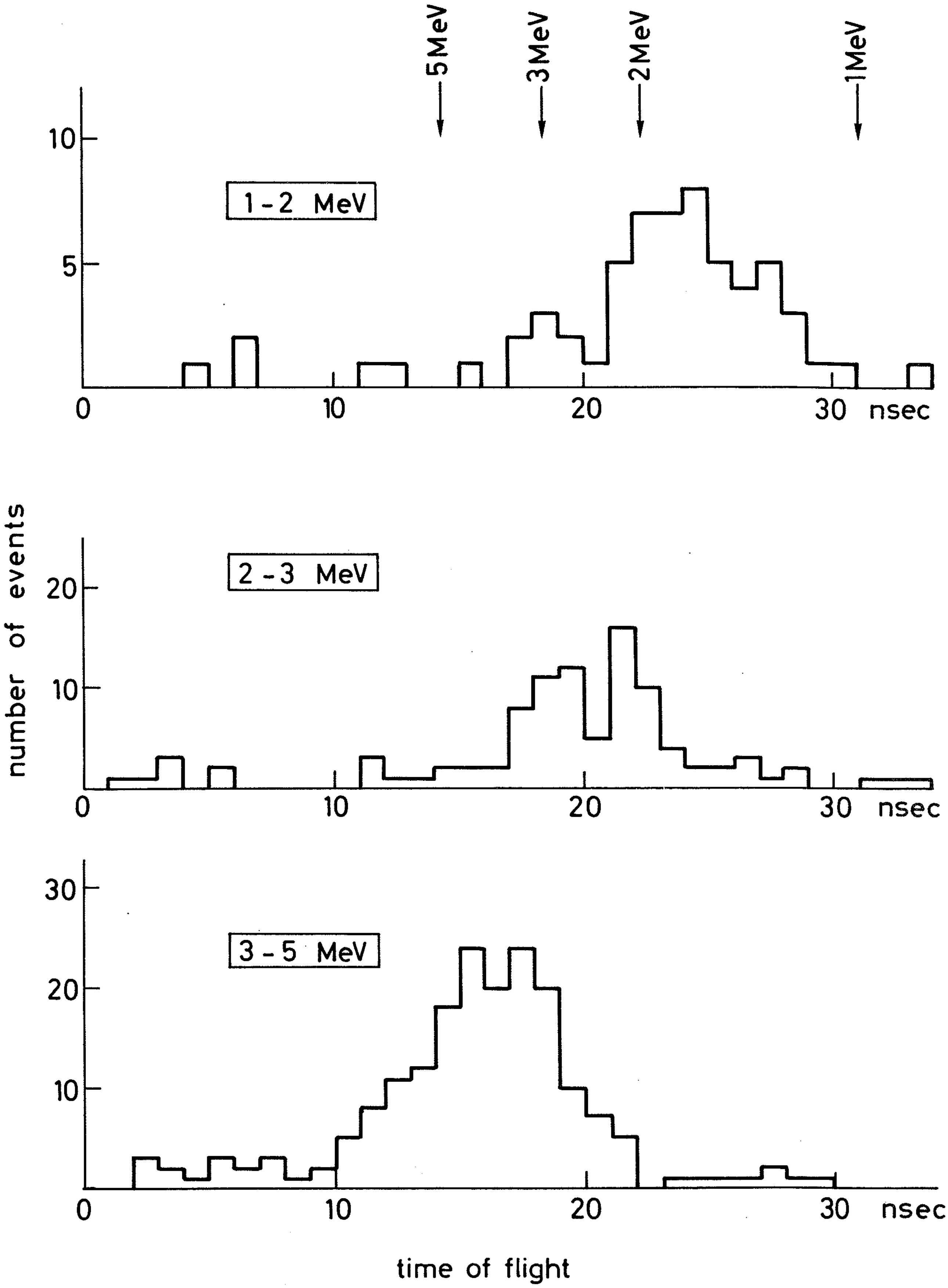
5MeV
3MeV
2MeV
1MeV
1-2 MeV
2-3 MeV
3-5 MeV
number of events
10
5
20
10
30
20
10
0
10
20
30
nsec
time of flight

Fig. 7

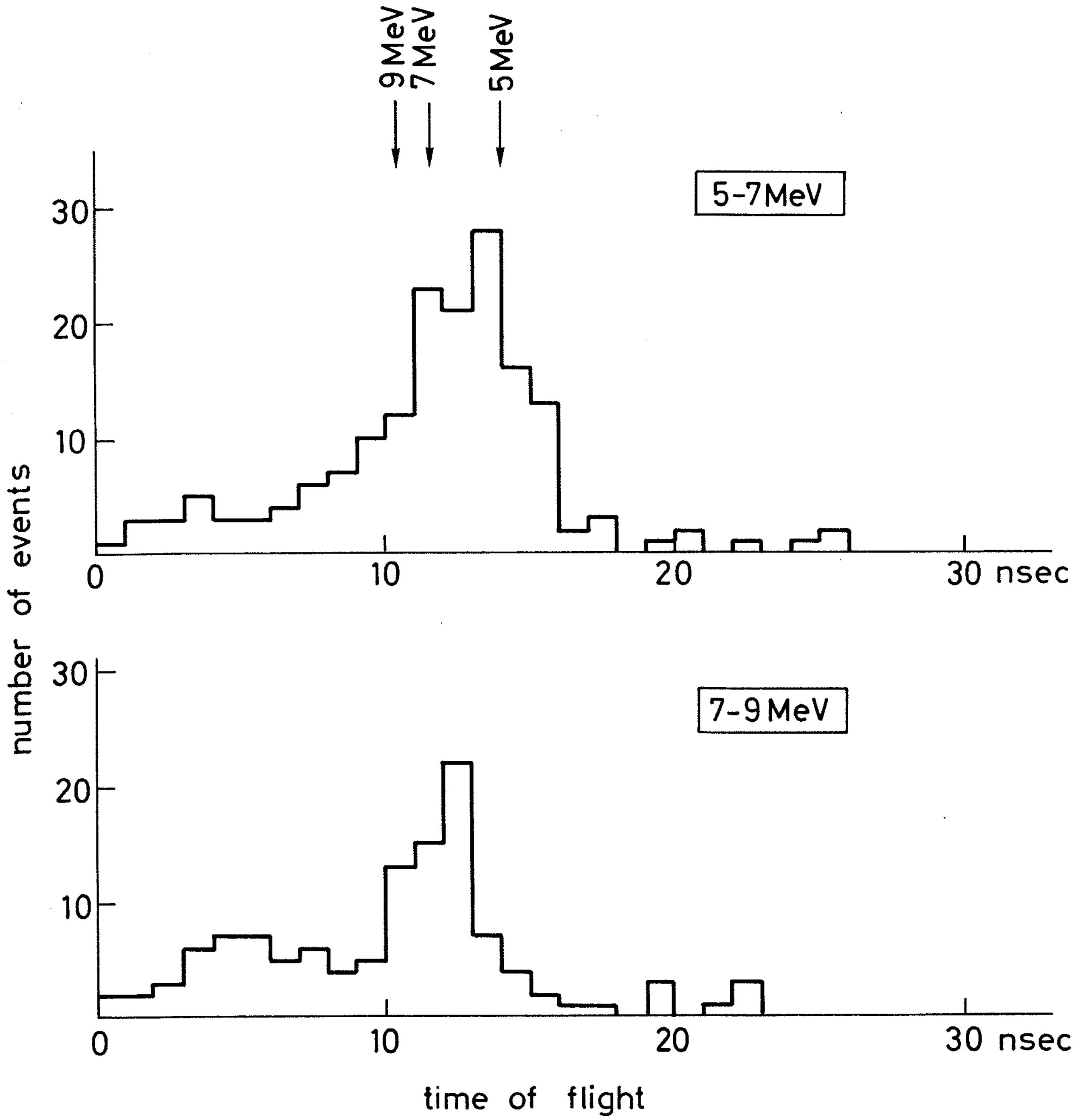
9 MeV
7 MeV
5 MeV
5-7MeV
7-9 MeV
30
20
10
0
10
20
30 nsec
number of events
time of flight

Fig. 8

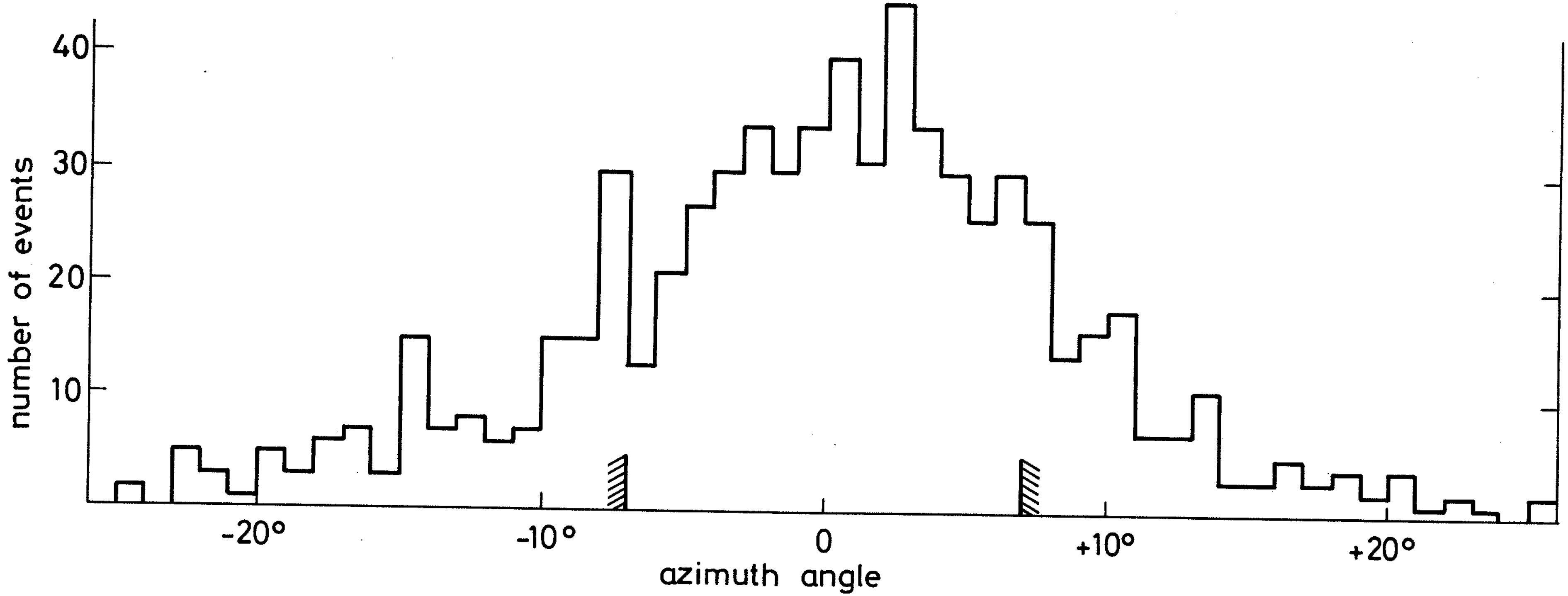

Fig. 9